Arch. Metall. Mater. **64** (2019), 4, 1549-1554

DOI: 10.24425/amm.2019.130125

P. PETRZAK*#, I. MANIA*, H. PAUL*, Ł. MAJ*, A. GAŁKA**

THE KINETIC OF Al_3Ti PHASE GROWTH IN EXPLOSIVELY WELDED MULTILAYERED Al/Ti CLADS DURING ANNEALING UNDER LOAD CONDITIONS

Multilayered composites based on light metals are promising materials in many applications. In the present work the 15-layered clad, composed of alternately stacked of Ti(Gr.1) and AA1050-H24 alloy sheets of 1 mm thick has been investigated with respect to determination of the kinetic of the Al_3Ti phase growth. The defect-free multilayered composite was successfully formed by explosive welding technology. Then EXW samples were modified *via* annealing at the temperature of 600°C in closed die under pressure of 44 MPa for various times ranged between 1 and 10 h. Transmission and Scanning Electron Microscopy examinations were conducted in order to study the kinetic of the elements migration across the interfaces between the layers of the Al/Ti composite. The macro-scale observations of samples after EXW revealed that wavy interfaces were always formed in layers near the explosive charge. The increase of the distance from the top surface leads to flattening of the interface with very thin reaction layer between Al and Ti sheets. During annealing the kinetic of the Al_3Ti phase growth is similar near all interfaces and coincides with data from other works. It was found that despite the loading after 10 h of annealing still only small part of Al-sheets undergoes dissolution and the width of the reaction layer does not exceed 5-8 μm.

Keywords: Explosive welding, annealing under compression, Al/Ti multilayered composites, Al_3Ti phase

1. Introduction

In the past few decades, rapid development of the multilayered composites has been observed. Increased interests in these materials is associated with the improvement of mechanical properties of the cladded components with respect to parent materials [1,2].

Various combinations of laminated composites including: metal-metal [2], metal-intermetallic [3], ceramic-ceramic [4] and metal-ceramic [5] possess improved high specific strength, corrosion resistance and fatigue characteristic. This turns those materials attractive in terms of application, especially intermetallic-metallic composites with its potential application in automotive and aerospace but also for military industry [6]. Those components are commonly labeled as hybrid materials [7]. The composite materials reinforced by the hard phases are especially suggested for potential industrial applications as materials exhibiting a high ballistic resistance. They can be used for the protection of people, vehicles and buildings, from not only ballistic impact but also different ones originating from other high impact risks. In order to fabricate desired composite composed of dissimilar materials few methods of solid state joining processes are being used [8], mainly: friction stir welding [9], explosive welding [10,11]. However, nowadays only explosive welding (EXW) opens the possibility to produce large, full-sized plated coatings of different thickness.

EXW method is defined as solid state joining process, which enables to join metals that are impossible or difficult to join *via* any other joining technique [12,13]. The process may be performed using parallel or inclined geometry with a stand-off distance between the plates [14,15]. The detonation of the explosive charge generates extreme pressure and leads to rapid increase of the temperature near the collision point. The very short time of the heat influence during explosion hinder the transfer of heat into the component metals [16]. Therefore, the melted metals exhibit a strong tendency to form brittle crystalline or amorphous phases during the solidification. Simultaneously, the interfacial layers of bonded metals undergo severe plastic deformation forming nano-grained structures.

From the wide spectrum of multilayered clads a special attention should be brought to the Al/Ti metals composition, which is characterized by high ratio of strength to weight and unique heat and oxidation resistance [17]. In the past the Al/Ti multilayered clads were successfully fabricated with the use of EXW technology, tailored mainly through the parallel geometry route, e.g. [18]. It has been revealed that the melted zones formed just after bonding near the interface consists of very fine-grained, crystalline or amorphous intermetallic phases, e.g. [6].

* INSTITUTE OF METALLURGY AND MATERIALS SCIENCE PAS, 25 REYMONTA STR., 30-059 KRAKOW, POLAND
** ZTW EXPLOMET, 100H OŚWIĘCIMSKA STR., 45-641 OPOLE, POLAND
# Corresponding author: p.petrzak@imim.pl

One of the significant advantages of the clads produced by this technology is that the structure of the joint can be easily 'modified' in further thermal treatment operations by creating layers of high hardness in areas near-the-interface. This makes it possible to fabricate materials of a laminar structure and significantly improved properties due to formation of the thin layers composed of intermetallic phases *via* elements diffusion across the interface. However, several problems connected with the porosity of the phases formed during annealing in air or in vacuum are noted. One of the way to solve this problem is annealing at the elevated temperatures under load. The growth kinetics during annealing in vacuum of Ti/Al laminar composites obtained with the use of EXW technology, were analysed in earlier works, e.g. by Fronczek et al. [6] in the 3-layered composite or by Lazurenko et al. [18] in 40-layered composite. There is scares amount of works examining the influence of the load during annealing on the kinetic of intermetallic phases growth in the Ti/Al clad [10].

Therefore, the aim of this work is to investigate the growth kinetics of the intermetallic phases in the 15-layered multilayered clad obtained by EXW method during annealing under compression. The analysis were provided by means of transmission (TEM) and scanning (SEM) electron microscopies, whereas the welding conditions were tailored through the parallel geometry route.

2. Materials and methodology

The explosive welding of 15-layered Ti/Al clad, composed of alternately situated Al (AA1050-H24 alloy) and Ti(Gr.1) sheets was performed by ZTW Explomet (Opole, Poland) with the use of parallel geometry route. Sheets with a thickness of 1 mm were used to 'build' the clad. The top and bottom layers of the clad were made of Ti. The plate's size was 210×300 mm. The contact surfaces of the joined plates were ground, cleaned of solid contaminants and degreased. A detonator was located in the middle of the shorter edge of the flyer plate, whereas the stand-off distance between sheets was 1 mm. A modified Saletrol explosive charge was applied in order to obtain detonation velocity of 2600 m/s; a measuring instrument Explomet-Fo-2000 (by Kontinitro) was used to measure detonation velocity. The plates in the initial state were characterized by a uniform, fully recrystallized microstructure. The analysed cross-sections perpendicular to the rolling plane of the Ti sheet have nearly equiaxed grains, whereas in the AA1050-H24 alloy plate the flattened grains were observed. Chemical composition and mechanical properties of used materials is given in Table 1.

Samples with dimensions of 15 mm×15 mm were cut-off from the middle section of the clad, then subjected to the compression under load of 10 kN (in the air atmosphere) at the temperature of 600^{o}C for a times: 1 h, 2 h, 5 h and 10 h. The experiment was conducted using the testing machine – Zwick-Roell Z1200, equipped with a heating chamber. The closed matrix preventing the flow of aluminum during the compression at high temperature was used. After heat treatment samples were cut into halt using precision wire saw. In order to obtain mirror-finished cross-sections a standard grinding technique was applied to both initial and compressed samples as well as polishing with the use of silica suspension mixed with diamond polishing suspensions.

Microstructure observations of near the interface layers of the initial (after EXW) and annealed samples were carried out using a scanning electron microscope (SEM) PHILIPS XL30 operating at the accelerating voltage 15 kV and working distance of 6 mm. The SEM was equipped with backscattered electrons (BSE) detector and LINK ISIS energy dispersive X-ray spectrometer (EDX). The width of the intermetallic phases layers were measured with a dedicated computer program. The microstructure observations in nano-scale were carried out using a transmission electron microscopy (TEM) employing FEI Technai Super TWIN G2 FEG operating at 200 kV, equipped with an EDAX energy dispersive X-ray (EDX) microanalysis system. Electron transparent thin foils were obtained from selected regions from the upper interface and prepared by the focused ion beam instrument technique using FEI Quanta 3D Dual Beam Focused Ion Beam (FIB).

3. Results and discussion

3.1. Macro- and micro-scale observations

Macro-scale observations carried out on the post-bonded plates revealed heterogeneous nature of the joint across the thickness. The phenomenon of rapid solidification of the melted zones at the interface, caused by the high impact energy during explosive welding process followed by extremely high cooling, created areas with indirect Z-contrast compared to the base materials (Fig. 1). For the first interface (near the explosive charge) the wavy nature of the joint was observed with the melted zones located in the vortexes. Remaining joints exhibited flat character

TABLE 1

Chemical composition (wt. %) and mechanical properties of welded materials

Alloy	C	N	O	H	Cu	Mg	Si	Fe	Mn	Zn	Ti
Ti Gr. 1	<0,08	<0,03	<0,18	<0,015	—	—	—	<0,2	—	—	—
Al 1050-H24	—	—	—	—	<0,05	<0,05	<0,25	<0,4	<0,05	<0,07	<0,05

Alloy	Hardness (HBW)	Tensile Strength (MPa)	Yield Strength (MPa)	Modules of Elasticity (GPa)
Ti Gr. 1	120	240	170	105
Al 1050-H24	33	145	84	68

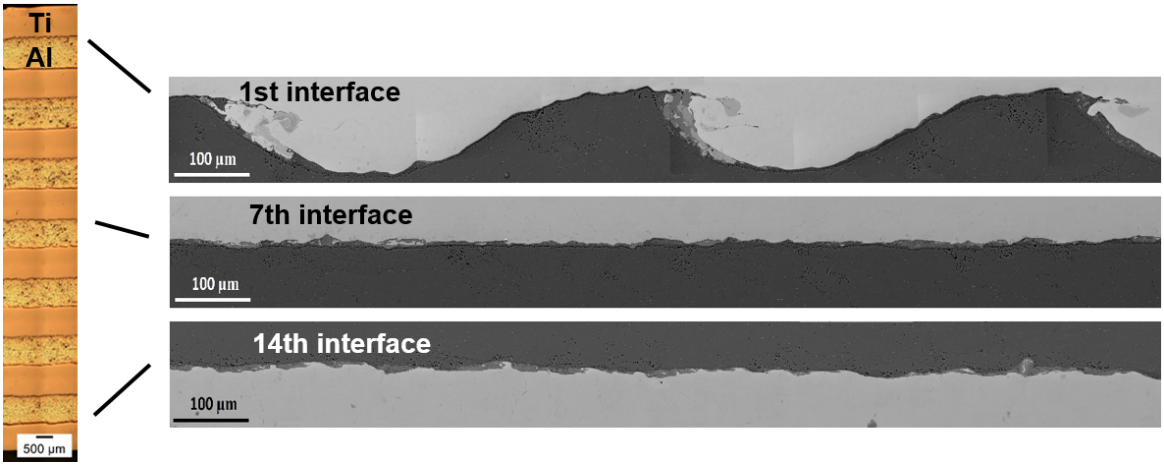

Fig. 1. Cross-section of welded Ti/Al multilayer composite showing overview of the sample cross-section (left) and details of 1st, 7th and 14th interface (right)

with melted zones in the form of thin and (semi)continuous layers. Detailed analysis in the micro-scale reveals the formation of a thin, continuous reaction layer between the plates. In all cases, SEM images revealed a sharp transition between melted zones and base materials (Fig. 2), i.e. presenting different Z-contrast in SEM/BSE images. This indicates significant chemical composition changes across the interface.

The SEM/EDX analysis carried out to determine the local chemical composition changes revealed that the content of Ti and Al in given area inside the respective melted zones varied significantly. In the case of a melted zone located along the first interface, the concentration of the main elements varies considerably depending on changes in the Z-contrast. The measured concentration of Ti varies from 29 to 70 at. %, while Al – from 71 to 30 at. % (points of SEM/EDX spot analysis are shown in the Fig. 2). Relatively small differences of chemical composition on other interfaces (measurements for the 7th and 14th interface) were observed. It has been found that Ti variation is ranged between 19 and 24 at. %, while Al between 76 and 81 at. %. In the 'after bonding' state, mainly the non-equilibrium phases were identified in the melted zones, i.e. the phases not observed on the Al-Ti phase equilibrium diagram. However, small areas with a chemical composition corresponding to the four equilibrium phases, i.e. $TiAl_3$, $TiAl_2$, TiAl and Ti_3Al, have also been identified.

After annealing, all the above phases identified inside the melted zones were transformed into the Al_3Ti phase. The existing phases transformation coincides with the initiation of elements diffusion across the interface towards neighboring layers; this leads to the formation of new intermetallic layers and growth the existing one. Regardless of the time applied in the process, continuous layer of Al_3Ti phase was formed, the width of which increased with the annealing time. Significant variation in the growth rate of the Al_3Ti phase on the thickness of the clad was observed. The effect was correlated with the structural diversity in the post-bonded state. Figure 3 presents the microstructure of the intermetallic layer formed on the 7th interface for four heat treatment variants. The width of the layer varies from about 1 µm for annealing time 1 h to 5 µm for annealing time 10 h.

3.2. Nano-scale observation

The TEM/BF microstructure observations of as-welded Ti/Al multilayered clad with a flat interface revealed that the plastic deformation resulted from EXW process caused the formation of large amount of defects in the base plates (Fig. 4a). At the interface between parent materials, the melted zone in the form of thin continuous layer was formed. The indexation of the selected area diffraction (SAED) pattern allowed to state

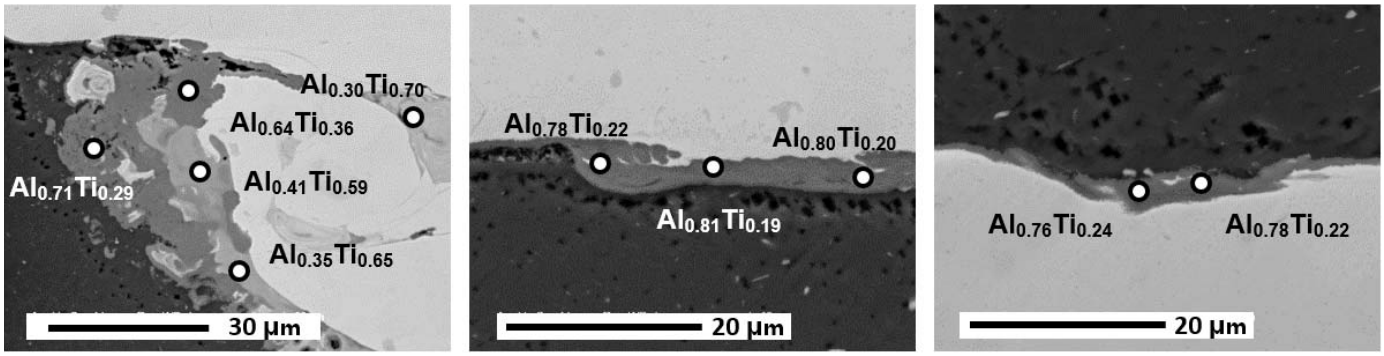

Fig. 2. SEM/BSE images presenting a) 1st, b) 7th and c) 14th interface of explosive welded Ti/Al multilayer

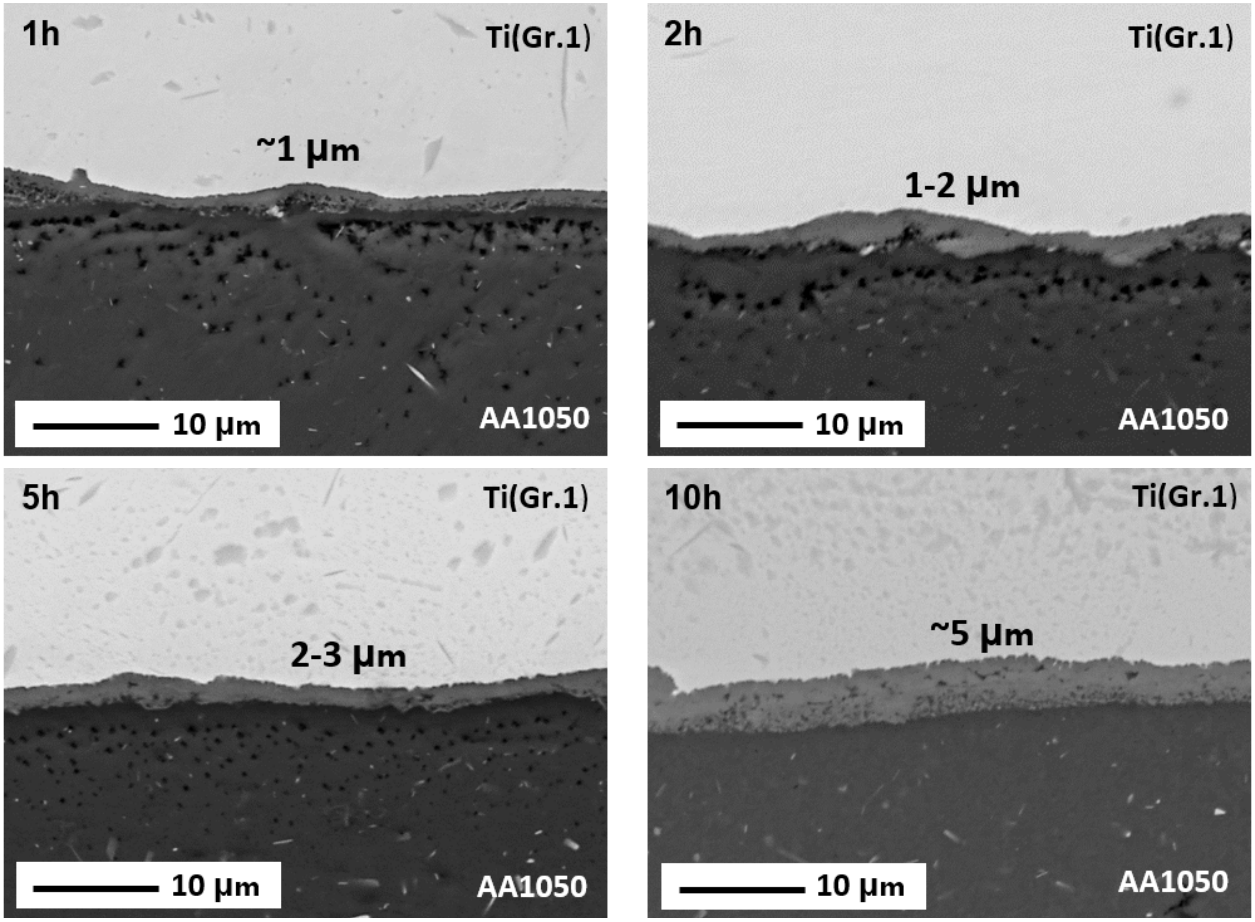

Fig. 3. SEM/BSE images presenting impact of annealing time on width of the intermetallic phase

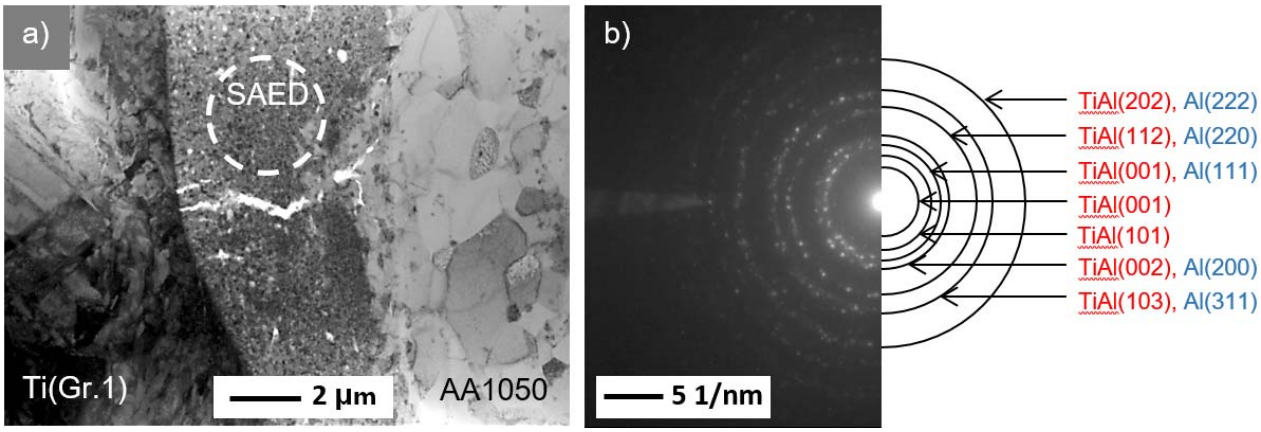

Fig. 4. TEM/BF microstructure image of the flat part of the interface of as-welded Ti/Al multilayer clad (a) and corresponding the SAED pattern acquired near to the interface between parent materials (b)

that the melted zone consists of Al and TiAl grains (Fig. 4b), as already characterized with TEM/BF method [19].

The TEM bright field images of Ti/Al multilayered clad annealed at 600°C for 1 h and 10 h under load of 44 MPa (in air) are presented in Fig. 5. The heat released during welding and supported by further annealing led to the recrystallization of the AA1050-H24 material and to the formation of defect-free aluminum grains, as presented in Fig. 5a. Due to much higher melting point of Ti some structural defects in the area near the interface may be observed. The heat treatment of the clad also resulted in the formation of a continuous layer between joined sheets of Ti and Al with the average thickness varied from 1 µm up to 10 µm for 1 h and 10 h of annealing times, respectively (Figs. 5a,c). The microstructure observations carried out at higher magnifications revealed the presence of both columnar and equiaxed grains of newly formed phase within diffusion zone. The average grain size of this phase was determined to be ~400 nm. Indexing of SAED pattern, obtained from the area

marked in Fig. 5a with dashed circle, allowed to state that the diffusion zone is composed of crystallites composed of the Al_3Ti intermetallic phase (Fig. 5d).

It should be noted that the Al_3Ti intermetallic phase was the only phase developed at the interfaces of Ti/Al multilayered clad. The same Al_3Ti intermetallic phase formation was observed at each Ti/Al interface during annealing of explosively welded multilayered Al/Ti clads by Bataev et al [10]. In that case the diffusion zone was filled with only equiaxed grains with a size exceeding 1 μm. The grain size of Al_3Ti phase is larger than

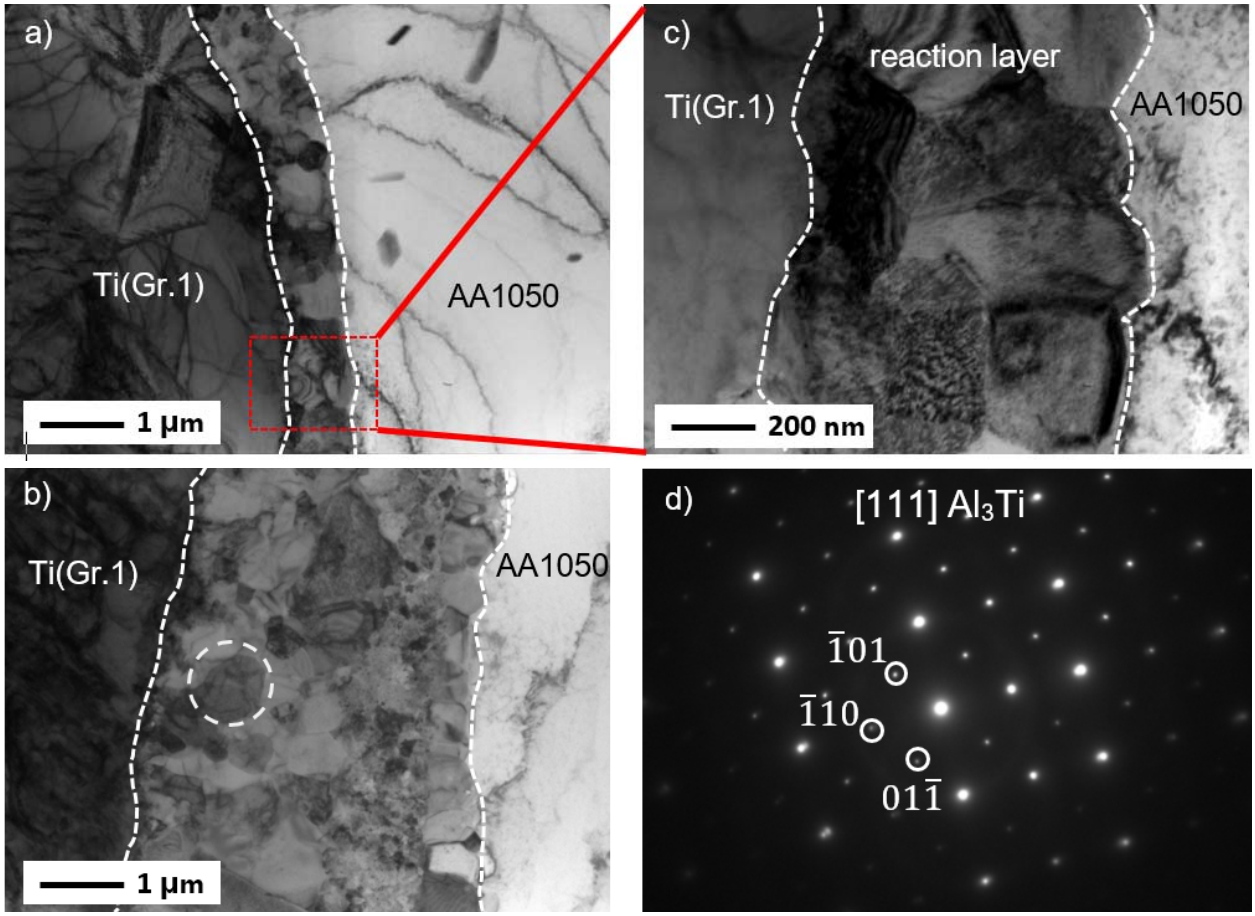

Fig. 5. TEM/BF microstructure images of Ti/Al multilayer clads obtained through explosive welding and annealed at 600°C for 1 h (a, b) and 10 h (c) under a load of 44 MPa, and corresponding SAED pattern obtained from reaction layer (marked by dashed circle) (d)

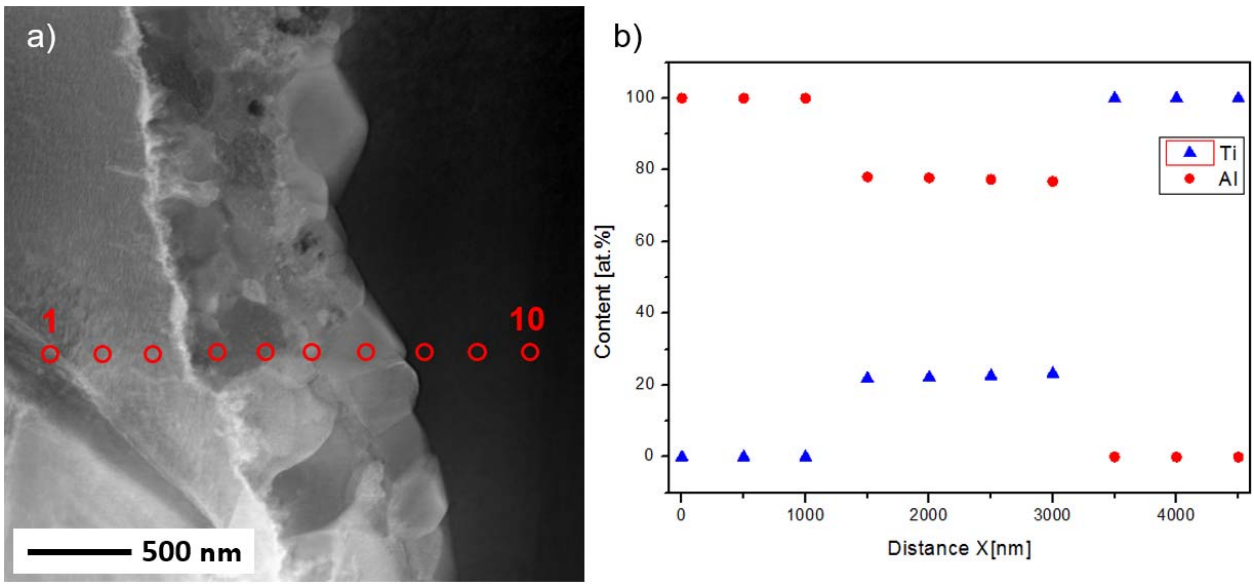

Fig. 6. STEM/HAADF microstructure image of explosively welded and annealed Ti/Al multilayer clad (a) and chemical composition line scan measured across the Ti/Al interface by TEM/EDX (b)

obtained in present work, as the TEM sample was cut-off from the clad annealed for longer annealing times. TEM/EDX analysis of chemical composition, carried out across the Ti/Al interface (as presented in Fig. 6a) revealed a gradual decrease in the content of Al and Ti. The measurements showed that the reaction between Ti and Al led to the formation of the diffusion zone in the form of continuous layer containing ~77 at. % of aluminum and ~23 at. % of Ti, what corresponds to the Al_3Ti intermetallic phase (Fig. 6).

4. Conclusions

Observations carried out on clads in the state 'after bonding' have shown the heterogeneous nature of the zones of solidified melt composed, mainly of non-equilibrium phases. However, small areas with a chemical composition similar to the four equilibrium phases, i.e. $TiAl_3$, $TiAl_2$, TiAl and Ti_3Al, have also been revealed. During annealing, all the above phases identified in the melted zones were transformed to the Al_3Ti phase. Regardless of the applied annealing time, the experiment documents the formation of a continuous layer of Al_3Ti phase, the width of which increases with increasing time of annealing.

Acknowledgements

This work was partially supported by the Polish National Centre of Science (NCN), project no.: UMO-2016/21/B/ST8/00462. The authors would like to take this opportunity to express their appreciation.

REFERENCES

[1] R. Wuhrer, M. Lee, K. Moran, Y. Yeung, Microchim. Acta **30**, 225-230 (2006).
[2] X. Peng, R. Wuhrer, G. Heness, W. Yeung, J. Mater. Sci. **34**, 2029-2038 (1999).
[3] D.J. Harach, K.S. Vecchio, Metall. Mater. Trans. A **32**, 1493-1505 (2001).
[4] W.J. Clegg, Acta Metall. Mater. **40**, 3085-3093 (1992) .
[5] K. Hwu, B. Derby, Acta Mater. **47**, 545-563 (1999).
[6] D.M. Fronczek, R. Chulist, Z. Szulc, J. Wojewoda-Budka, Mater. Lett. **198**, 160-163 (2017).
[7] T. Sapanathan, S. Khoddam, S.H. Zahiri, J. Alloy Compd. **57**, 85-92 (2013).
[81] M. Kaczorowski, O. Goroch, A. Krzyńska, Arch. of Found. Eng. **14**, 37-42 (2014).
[9] M. Fazel-Najafabadi, S.F. Kashani-Bozorg, A. Zarei-Hanzaki, Mater. Des. **31**, 4800-4807 (2010).
[10] A. Bataev, V. Bataev, D. Mali, Pavliukova, Mater. Des. **35**, 225-234 (2012).
[11] B. Gulenc, Mater. Des. **29**, 275-278 (2008) .
[12] P. Mikell Groover (Ed.), Fundamentals of Modern Manufacturing: Materials, Processes, and Systems, Wiley **4**, 734-735 (2010).
[13] T. T. Zhang, W. X. Wang, J. Zhou, X. Q. Cao, Z. F. Yan, Y. Wei, W. Zhang, J. Mater. **70** (4), 504-509 (2018) .
[14] H. Paul, M.M. Miszczyk, R. Chulist, M. Prażmowski, J. Morgiel, A. Gałka, M. Faryna, F. Brisset, Mater. Des. **153**, 177-189 (2018).
[15] F. Grignon, D. Benson, K.S. Vecchio, M.A. Meyers, Int. J. Imp. Eng. **30**, 1333-1351 (2014).
[16] F. Findik, Mater. Des. **32**, 1081-1093 (2011).
[17] D.M. Fronczek, J. Wojewoda-Budka, R. Chulist, A. Sypien, A. Korneva, Z. Szulc, N. Schel, P. Zieba, Mater. Des. **91**, 80-89 (2016).
[18] D.V. Lazurenko, I.A. Bataev, V.I. Mali, A.A. Bataev, I.N. Maliutina, V.S. Lozhkin, M.A. Esikov, A.M.J. Jorge, Mater. Des. **102**, 123-130 (2016).
[19] J. Wojewoda, P. Zięba, B. Onderka, R. Filipek, P. Romanów, Arch. Metall. Mater. **51** (3), 345-352 (2006).